CHEMMEDCHEM

CHEMISTRY ENABLING DRUG DISCOVERY

Accepted Article

Title: An angle on MK2 inhibition - Optimization and evaluation of prevention of activation inhibitors

Authors: Mickael Tommy Mogemark, Ulf Hedström, Monica Norberg, Emma Evertsson, Sarah R. Lever, Magnus Munck af Rosenschöld, Hans Lönn, Peter Bold, Helena Käck, Pia Berntsson, Johanna Vinblad, Jianming Liu, Anette Welinder, Johan Karlsson, Arjan Snijder, Katerina Pardali, Ulf Andersson, and Andrew M. Davis

To be cited as: *ChemMedChem* 10.1002/cmdc.201900303

Link to VoR: http://dx.doi.org/10.1002/cmdc.201900303

A Journal of

ChemPubSoc Europe

WILEY-VCH

www.chemmedchem.org

WILEY-VCH

FULL PAPER

An angle on MK2 inhibition - Optimization and evaluation of prevention of activation inhibitors

Ulf Hedström,[b] Monica Norberg,[b] Emma Evertsson,[b] Sarah R. Lever,[b] Magnus Munck af Rosenschöld,[b] Hans Lönn,[b] Peter Bold,[b] Helena Käck,[c] Pia Berntsson,[b] Johanna Vinblad,[b] Jianming Liu,[c] Anette Welinder,[d] Johan Karlsson,[c] Arjan Snijder,[c] Katerina Pardali,*[b] Ulf Andersson,[a] Andrew M. Davis,[b] Mickael Mogemark*[a]

Dedicated to Ulrika Svensson

[a] Dr. Mickael Mogemark (https://orcid.org/0000-0002-7484-3719), Dr. Ulf Andersson
Clinical Pharmacology and Safety Sciences, R&D Biopharmaceuticals, AstraZeneca, Gothenburg, Sweden
Pepparedsleden 1, 431 83 Mölndal, Sweden
E-mail: mickael.mogemark@astrazeneca.com

[b] Dr. Ulf Hedström, Dr. Monica Norberg, Dr. Emma Evertsson, Sarah R. Lever, Magnus Munck af Rosenschöld, Dr. Hans Lönn, Dr. Peter Bold, Pia Berntsson, Johanna Vinblad, Dr. Katerina Pardali (https://orcid.org/0000-0002-4360-730X), Dr. Andrew M. Davis
Early Respiratory, Inflammation and Autoimmunity, R&D Biopharmaceuticals, AstraZeneca, Gothenburg, Sweden
Pepparedsleden 1, 431 83 Mölndal, Sweden
E-mail: : ulf.hedstrom@astrazeneca.com, emma.evertsson@astrazeneca.com, peter.bold@astrazeneca.com, pia.berntsson@astrazeneca.com, katerina.pardali@astrazeneca.com, andy.davis@astrazeneca.com

[c] Dr. Helena Käck, Dr. Jianming Liu, Johan Karlsson, Dr. Arjan Snijder
Discovery Sciences, R&D Biopharmaceuticals, AstraZeneca, Gothenburg, Sweden
Pepparedsleden 1, 431 83 Mölndal, Sweden
E-mail: helena.kack@astrazeneca.com, jianming.liu@astrazeneca.com

[d] Anette Welinder
Pharmaceutical Technology and Development, Operations, AstraZeneca, Gothenburg, Sweden
Pepparedsleden 1, 431 83 Mölndal, Sweden
E-mail: anette.welinder@astrazeneca.com

Abstract: The mitogen-activated protein kinase p38α pathway has been an attractive target for the treatment of inflammatory conditions such as rheumatoid arthritis. While a number of p38α inhibitors have been taken to the clinic they have been limited by their efficacy and toxicological profile. A lead identification program was initiated to selectively target prevention of activation (PoA) of mitogen-activated protein kinase-activated protein kinase 2 (MK2) rather than mitogen- and stress-activated protein kinase-1 (MSK1), both immediate downstream substrates of p38α, to improve the efficacy/safety profile over direct p38α inhibition. Starting with a series of pyrazole amide PoA MK2 inhibitor leads, and guided by structural chemistry and rational design, a highly selective imidazole **9** and the orally bioavailable imidazole **18** were discovered. The PoA concept was further evaluated by protein immunoblotting, which showed that the optimized PoA MK2 compounds, despite their biochemical selectivity against MSK1 phosphorylation, behaved similarly to p38 inhibitors in cellular signaling. This study highlights the importance of selective tool compounds in untangling complex signaling pathways, and while **9** and **18** were not differentiated from p38α inhibitors in a cellular context, they still are useful tools for further research directed to understand the role of MK2 in the p38α signaling pathway.

Introduction

The mitogen-activated protein kinases (MAPK) p38α MAPK (p38α) and MAPK-activated protein kinase 2 (MK2) are attractive drug discovery targets for the treatment of inflammatory conditions such as rheumatoid arthritis (RA).[1],[2],[3] Several p38α inhibitors have been tested in the clinic for rheumatoid arthritis including BIRB796 (BI),[4] VX-745[5] and VX-702 (Vertex)[6], but were discontinued due to concerns over their toxicological profile and/or lack of efficacy at the doses that could be used.[7] Selectively targeting MK2 downstream of p38α has been suggested to provide p38α-like efficacy with downregulation of TNF-α production along with an improved safety profile.[3],[8] The interest in selectively targeting MK2 also resides in the fact that p38α not only activates MK2 but also mitogen- and stress-activated protein kinase 1 (MSK1). The inhibition of MSK1 leads to downregulation of the anti-inflammatory cytokines interleukin (IL)-10 and IL-1 receptor antagonist (IL-1RA) and hence reduction of the overall efficacy.[8] We hypothesized that a ligand selectively binding to the heterodimeric complex of p38α/MK2 could block the production of pro-inflammatory TNF-α, whilst maintaining the IL-10 and IL-1RA levels (Figure 1).

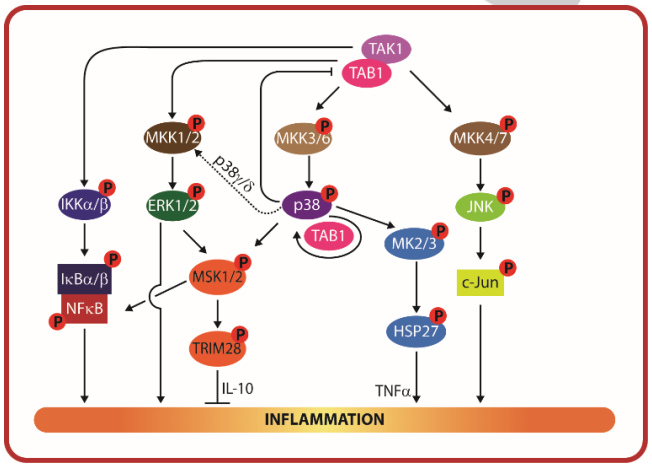

Figure 1. Schematic representation of MAP kinase signaling network.

Furthermore, we aimed at inhibiting the phosphorylation of MK2 by binding to the heterodimeric complex of p38α/MK2 via a prevention of activation (PoA) mechanism.[9],[10] Hence, the inhibition should be substrate selective since it wouldn't interfere with the p38α-MSK1 signaling as described previously.[10] High throughput screening of the AstraZeneca compound collection afforded two distinct lead series represented by hit compounds **1** (series 1) and **2** (series 2) , showing a promising separation of p38α-MSK1 substrate selectivity (Figure 2).[10] In this paper we describe our efforts to further explore the pyrazole amide series 2, evolved from compound **2**.

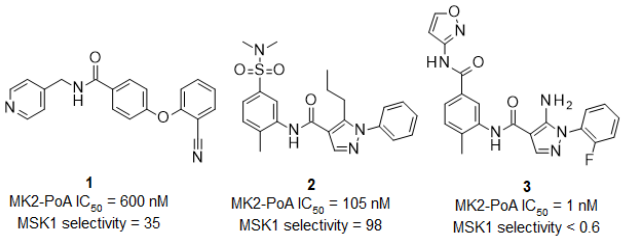

Figure 2. AstraZeneca high throughput screening hit compounds **1-2** and compound **3** from Bristol-Myers Squibb targeting p38α.

Results and Discussion

The p38α inhibitor **3**, previously disclosed by Das et al,[11] is structurally similar to compound **2**, but while **2** is 98x selective for MK2 inhibition over MSK1, **3** is not selective (Figure 2). In order to understand the selectivity profile of **2**, it was crystallized in complex with p38α/MK2, and its binding interactions compared to **3**. The X-ray of **2** bound to p38α/MK2 (pdb code: 4THY) shows that it can bind to the ATP binding pocket of p38α (Figure 3a). The binding of **2** to the p38α/MK2 complex displays hydrogen bond interactions between the sulfonamide oxygen and the Asp168 backbone NH, and between the pyrazole nitrogen and the hinge residue Met109. The n-propyl substituent does not appear to make any specific interaction and leaves room for further modification of this substituent. The pyrazole phenyl group reaches towards the MK2 protein surface in the protein complex however, the distance is too long for direct interactions (closest distance to Gln369 is 3.7 Å). The structurally analogous compound **3** displays similar binding interactions to p38α (Figure 3b), but without the sulfonamide oxygen interaction to Asp168, potentially responsible for driving the selectivity for PoA-MK2 versus PoA-MSK1. Compound **2** is a moderately potent inhibitor of MK2 but with good selectivity towards MSK1 through its specific interactions with the p38α/MK2 complex, but with low aqueous solubility and low stability in human liver microsomes. Hence, our design strategy was to improve the MK2-PoA potency and the drug-like properties, while improving selectivity towards MSK1 by building on the interactions made by **2** to the p38α/MK2 complex, and further extending towards the MK2 protein surface.

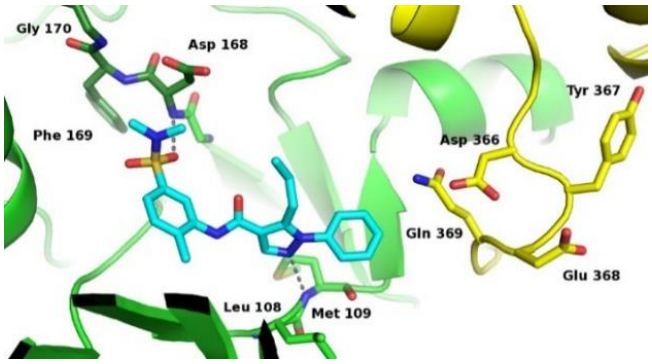

Figure 3a. Structure of compound **2** (cyan) binding to the p38α/MK2 complex. Gln369, Glu368, Tyr367 and Asp366 (shown to the right in yellow) are part of the MK2 chain of the complex. DFG loop residues Asp168, Phe169 and Gly170 are shown in dark green and the hinge residues Leu108 and Met109 are shown as bold sticks. Putative hydrogen bonds are shown as dashed lines. (pdb code: 4TYH).

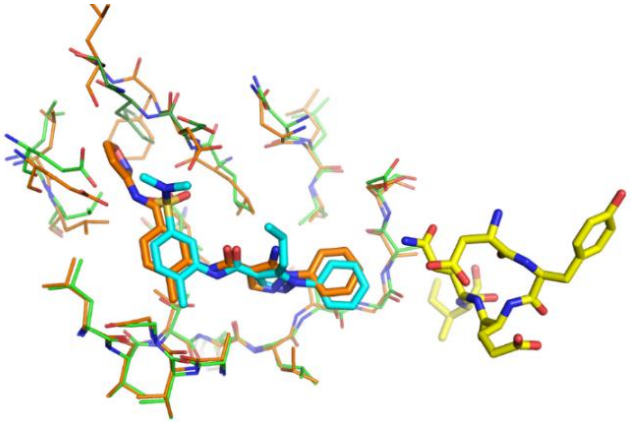

Figure 3b. Comparison of compound **3** (orange) binding to the active site of p38α (pdb code: 3OCG) and compound **2** (cyan) binding to the p38α/MK2 complex (p38α in green and MK2 in yellow) (pdb code: 4TYH).

Initial structure-activity relationship (SAR) investigation focused on identifying alternatives to the pyrazole core. The imidazole-based compound **4** (Table 1) offered an opportunity to maintain the key interaction with Met109 while exploring lipophilicity-dependent effects, e.g. solubility, and intrinsic clearance, and thereby improve the overall pharmacokinetic profile. The potency for the imidazole analogue **4** improved 2-fold in the MK2-PoA assay compared to its pyrazole analogue **2**. Despite equivalent LogD, the solubility of imidazole **4** was improved 70-fold compared to the corresponding pyrazole **2**. The importance of the sulfonamide in the aniline 5-position was confirmed by introducing different polar groups, preserving the possibility for a hydrogen bond interaction with Asp168 in the p38α/MK2 complex, as previously shown in the pyrazole series.[10] Changing the tertiary sulfonamide **4** to the primary sulfonamide **5** increased MK2-PoA potency, but with an overall drop in the MK2-PoA/MSK1-PoA selectivity. Replacing the sulfonamide with primary or secondary amides **6** and **7**, resulted in sub-nanomolar MK2-PoA potencies, but also led to a complete loss of selectivity over MSK1. The carboxylic acid **8** lost 6-fold in MK2-PoA potency with a 70-fold gain of selectivity over MSK1-PoA compared to amide **6**. Unfortunately, the carboxylic acid analogue **8** did not inhibit TNF-α production in lipopolysaccharide (LPS)-stimulated human peripheral blood mononuclear cells (PBMC) (data not shown). To further improve potency and selectivity, we extended the molecules towards the MK2 protein surface of the p38α/MK2 complex in an attempt to identify novel interactions (Figure 3a and 3b). With the X-ray structure of **2** bound to the p38α/MK2 complex as starting point, compounds reaching towards the MK2 protein surface were designed and synthesized. Structure based design suggested that the terminal phenyl acetamide substituent had the possibility to generate a hydrogen bond to the Asp366 from MK2 protein as can be seen in docking shown in figure 4, which lead us to include this substituent in a library to explore SAR. As predicted, these meta-substituted phenyl acetamides showed promising activity and selectivity profiles. The primary amide **9**, as well as the secondary amide **10**, showed slightly improved potency compared to unsubstituted **4**, but more importantly the selectivity over MSK1-PoA increased more than 3-fold. However, both compounds suffered from poor metabolic stability and low solubility. Compound **9** was tested in a pan kinase selectivity panel of 273 kinases and was not active against any kinase tested at 1 μM (Table S1 in the Supporting Information). The left hand R1 substituent was revisited to investigate if the structure–activity relationship (SAR) for the R2 = phenyl acetamide subseries is parallel to that of the R2 = H subseries. The secondary sulfonamide **11** showed low nanomolar MK2-PoA potency, but with decreased MSK1 selectivity compared to the tertiary sulfonamide **9**. A similar trend was seen for the primary sulfonamide **12**, which was 10-fold less selective against MSK1 compared to compound **10**, although an improved potency was obtained. The primary amide **13** showed excellent MK2-PoA potency (IC50 = 2 nM), but displayed no selectivity over MSK1, in comparison with **6**. Compounds **11** and **13** suffered from low solubility but showed improved metabolic stability in human liver microsomes compared to compound **9**.

In summary, parallel SAR was observed for the two different sub-series. Nonetheless, comparing compound **9** to the compound **4**, the combination of tertiary sulfonamide and primary m-phenylacetamide substitutions afforded an apparent cooperative effect to improve MK2 selectivity over MSK1. This selectivity data supports the idea that substrate selectivity can be improved by extending towards the MK2 surface in the protein dimer complex, as suggested by docking studies.[12] These studies suggest the formation of a possible hydrogen bond between the NH of the phenylacetamide (R2-substituent) and Asp366 in the MK2 protein (Figure 4).

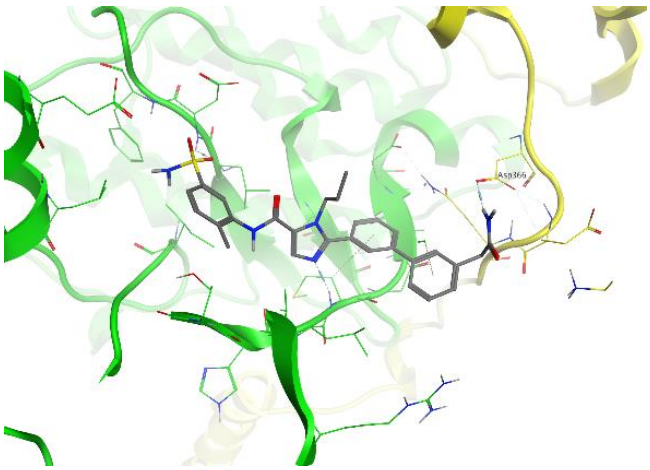

Figure 4. Docking of compound **9** into the p38α/MK2 tertiary complex, showing a potential H-bond between the terminal phenyl acetamide and Asp366 from the MK2 protein.

This interaction could potentially explain the observed increase in potency and selectivity. The sulfonamide substituent is remote from the MK2 and p38α interface, but close to the DFG motif which extends into the activation loop. Structural overlays between free and MK2-bound p38 suggest that the conformation of the p38 activation loop may be affected by interaction to MK2, and thus interactions with the DFG motif may have a significance for selectivity. However, we cannot yet explain the influence of the sulfonamide on selectivity in any details from the crystal structures or the docking studies.

To improve the overall pharmacokinetic profile with more ligand efficient compounds than found for the m-phenylacetamide subseries (most compounds showed both poor metabolic stability and solubility), we focused our attention on the core structure binding interactions and on modifications of the n-propyl chain in an attempt to improve LogD, solubility and metabolic stability. As was mentioned previously, the crystal structure of compound **2** in the p38α/MK2 complex (Figure 3), shows no apparent interaction between the n-propyl chain in compound **3** and the protein. We speculated that the propyl-chain is important for the conformation of the molecule, more precisely the torsional angle between the heteroaromatic core and the phenyl ring. This hypothesis prompted us to explore the conformational relationship, whilst trying to reduce size and lipophilicity of the propyl chain.

10.1002/cmdc.201900303

FULL PAPER

Table 1. Activity data for SAR exploration.

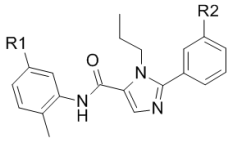

Compound	R1	R2	MK2-PoA IC_{50} (nM)[a]	MSK1 selectivity[b]	Octanol LogD[c]	Solubility (μM)[c]	HLM CL_{int} (μl/min/mg)[c],[d]
2[e]	Me_2NO_2S	H	105	98	3.6†	0.6†	62†
4	Me_2NO_2S	H	59†	53	3.5†	42	110
5	H_2NO_2S	H	19	10	2.7	280	26
6	H_2NOC	H	14	0.4	2.7	37	19
7	*c*PrHNOC	H	3.4	<0.5	3.5	8	<3
8	HO_2C	H	85‡	79	0.4	820	50
9	Me_2NO_2S	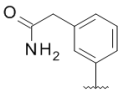	16†	270	3.8	0.5	>300
10	Me_2NO_2S	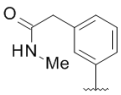	17‡	150	4.5	1	250
11	$MeHNO_2S$	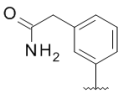	6.3†	95	3.5	5	95
12	H_2NO_2S	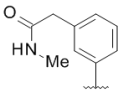	3.7‡	15	3.3	8	49
13	H_2NOC	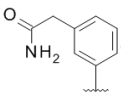	2.2†	1.5	3.1	0.5	5.4

[a] Values are means of n≥3, except †n=2 and ‡n=1. [b] MSK1-PoA IC_{50}/MK2-PoA IC_{50}. [c] Values represent n=1, except †n=2. [d] Intrinsic clearance (CL_{int}) in human liver microsomes (HLM). [e] Pyrazole heteroaromatic core.

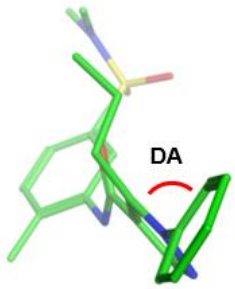

Figure 5. X-ray structure of compound **2** in the conformation that is bound to the p38α/MK2 complex, showing the dihedral angle between the pyrazole and phenyl.

The crystal structure of compound **2** bound to the p38α/MK2 complex shows a dihedral angle of ~60° between the pyrazole and the phenyl rings (Figure 5). For comparison, the crystal structure of the analogue p38α compound **3** (pdb code: 3OCG) shows a slightly larger dihedral angle of 66°. These measured values are significantly larger than the energy optimized dihedral angle of 20°, calculated using quantum mechanical geometry optimization (B3LYP/6-31G**)[13] for compound **2** and for the analogous compound **5**. This suggests that the binding to the protein increased the dihedral angle by 40°, corresponding to an energy penalty of about 7 kJ/mol. The dihedral angle of compound **3**, bearing an amine in 5-position on the imidazole, was also calculated. The angle was 53° with a 1 kJ/mol energy penalty to increase it to 60°. To identify substituents forcing a dihedral angle closer to the optimal angle of 60°, and thus maximize the binding free energy, we calculated the conformation of a molecule set. The set included simplified forms of N-methylated and unsubstituted imidazoles with different substituents in the 2-position of the adjacent phenyl (Table 2). The N-methylimidazole **18** with a methyl in the 2-positon on the phenyl provided a calculated dihedral angle of 64°. The energy cost of forcing the conformation to a dihedral angle of 60° was calculated to be 0.8 kJ/mol. A small set of compounds were subsequently synthesized including the non-methylated imidazoles as a control. To reduce the LogD and optimize bioavailability, we decided to focus on the primary sulfonamide on the aniline in this study.

In agreement with the calculations, compound **18** with a calculated dihedral angle of 64°, resulted in a 5-fold increase in potency compared to **5** (Table 3). In alignment with our predictions, the isopropyl substituted analogue **17** (126° dihedral angle) decreased the potency 20-fold in comparison to **18**. Three matching compounds with an unsubstituted imidazole were also prepared, **19**, **20** and **21**. All showed a complete loss in potency, which could be explained by the non-optimal dihedral angle varying between 7° and 20° (Table 2).

Table 2. DA is the calculated optimal dihedral angle between the imidazole and phenyl rings. ΔE is the energy (kJ/mol) required to force the dihedral angle to 60°. Substituents on the third, more distant ring were excluded from the calculations, since they are not expected to contribute to the dihedral angle.

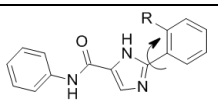

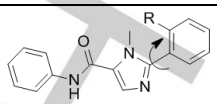

R	DA	ΔE (KJ/mol)	R	DA	ΔE (KJ/mol)
H	1	14	H	37	4.4
Me	7	9	Me	64	0.8
Et	18	7	Et	71	2.7
Pr	20	7	Pr	72	6.8
iPr	38	3	iPr	126	5.8
tBu	126	11	tBu	97	7.7
Ph	20	8	Ph	126	8.4

Table 3. Activity data for exploration of dihedral angle.

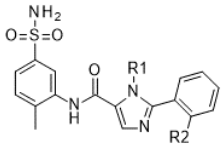

Compound	R1	R2	MK2-PoA IC_{50} (nM)[a]	MSK1 selectivity[b]
5	nPr	H	19	10
17	Me	iPr	61‡	5.8
18	Me	Me	3‡	22
19	H	Me	>990†	>3.6
20	H	Et	>990‡	>1.5
21	H	Ph	Not active†	-
3[c]			1	< 0.6

[a] Values represent n≥3, except †n=2 and ‡n=1. [b] MSK1-PoA IC_{50}/MK2-PoA IC_{50}. [c] Bristol-Myers Squibb Research and Development pyrazole core.

The described optimization of the dihedral angle focused on potency and physicochemical properties of the compounds, not taking the desired selectivity towards MSK1-PoA into account. The resulting compound **18** thus displayed excellent 3 nM potency for MK2-PoA but with a modest 22-fold selectivity. It also showed improved potency in the human PBMC cell assay (Table 4) compared to compound **9** and the lower LogD of 2.2 compared to 3.8 improved its properties for oral administration. Solubility was increased from 0.5 to 784 µM while clearance in human liver microsomes was reduced from >300 to <3 µl/min/mg. It was permeable with an apparent permeability value of 1.4 x 10^{-6} cm/s measured in Caco-2 cells, but exhibited an efflux ratio of 24, which might limit its absorption at low doses. However, despite promising in vitro data, compound **18** was cleared efficiently in rat with a clearance value of 37.4 ml/min/kg which corresponds to 51% of the liver blood flow (Figure S1 in the Supporting Information). To avoid more demanding in vivo studies, the in vitro-in vivo disconnect was not further pursued for these tool compounds at this stage of the project. Furthermore, compound **18** was inactive in a human ether-a-go-go-related gene (hERG) assay and in cytochrome P450 enzyme inhibition assays (5 isoforms) (data not shown). It was also tested in a pan-kinase selectivity panel of 130 kinases at 1 µM and showed excellent pan kinase selectivity (<31% inhibition against all kinases, except for p38α that showed 94% inhibition) (Table S2 in the Supporting Information).

Table 4. Biochemical and cellular potency profiles

p38 inhibitors:

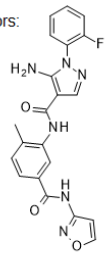

3

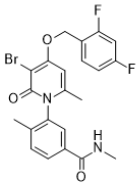

PH-797804

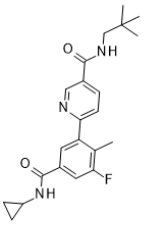

Losmapimod

MK2 inhibitors:

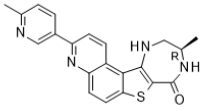

PF-3644022

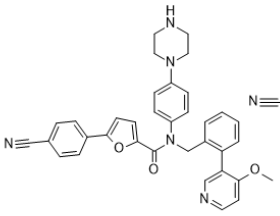

22

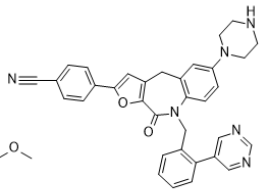

23

Compound	MK2-PoA IC_{50} (nM)[a]	MSK1 selectivity[b]	MK2 IC_{50} (nM)[c]	p38α IC_{50} (nM)[c]	Human PBMC TNF-α IC_{50} (nM)[a]	Human PBMC IL-10 IC_{50} (nM)[a]	IL-10 selectivity[d]
5	19	10	Not active	290	240†	1191†	5
9	16†	270	Not active	4600	1009	1874	1.9
18	3‡	22	Not active	83	119†	390†	3.2
3	1	< 0.6	15	Not active	1†	6.7†	6.7
PH-797804	2†	0.8	-	-	6	20	3.3
Losmapimod	10‡	0.5	Not active	-	8	27	3.4
PF-3644022	Not active	-	10	Not active	1128	1774	1.6
22	Not active	-	3	Not active	4540†	2583†	0.6
23	18500‡	-	4	Not active	55†	8485†	1.5

[a] Values are means of n≥3, except †n=2 and ‡n=1. [b] MSK1-PoA IC_{50} /MK2-PoA IC_{50}. [c] Values represent n=1. [d] IL-10 IC_{50}/TNF-α IC_{50}.

Despite good in vitro MSK1 selectivity, when compounds **5**, **9** and **18** were assessed in human PBMC after LPS stimulation, we were unable to detect the inhibition of TNF-α levels along with the preservation of IL-10 levels (Table 4).

In order to understand the effect of p38 inhibition, PoA MK2 inhibition and direct MK2 inhibition, we used protein immunoblotting to explore activation of pathways around p38 signaling (Figure 1). We analyzed phosphorylation of HSP27, TRIM28 and MSK1 as they are activated downstream of p38.[14],[15],[16] After stimulating human PBMC with LPS in the presence of the designated compounds at IC_{80} and 5 x IC_{80} concentrations of TNF-α inhibition, we observed that the known p38 inhibitors PH-797804,[17] Losmapimod[18] and **3** (Figure 6a) had a profile that was distinct from that of the MK2 active site inhibitors PF-3644022,[19] **22**[20] and **23**[21] (Figure 6b). The p38 inhibitors all inhibited p38 phosphorylation, completely abolished HSP27 phosphorylation and upregulated phosphorylation of ERK1/2 (Figure 6a). In contrast, the MK2 active site inhibitors PF-3644022, **22** and **23** upregulated p38 phosphorylation and partially inhibited HSP27 phosphorylation, while ERK1/2 phosphorylation was not induced (Figure 6b). The upregulation of p38 phosphorylation by MK2 inhibitors is in agreement with previous findings that suggest that inhibition of MK2 maintains p38 phosphorylation.[22] The mechanism for this relates to the ability of activated MK2 to regulate the export of p38 from the nucleus, which results in the dephosphorylation of p38 by cytosolic phosphatases.[23] When we investigated compounds **5** and **9** to understand if they behaved in a p38-like or MK2-like fashion, we observed that the compounds exhibited significant reduction of HSP27 phosphorylation, upregulated phosphorylation of ERK1/2, and no upregulation of p38 or MSK1 phosphorylation (Figure 6c). Compound **5** did not upregulate TRIM28 phosphorylation while compound **9** appeared to induce it. These results suggest that both compounds behave as p38-like inhibitors despite their biochemical selectivity against MSK1 phosphorylation.

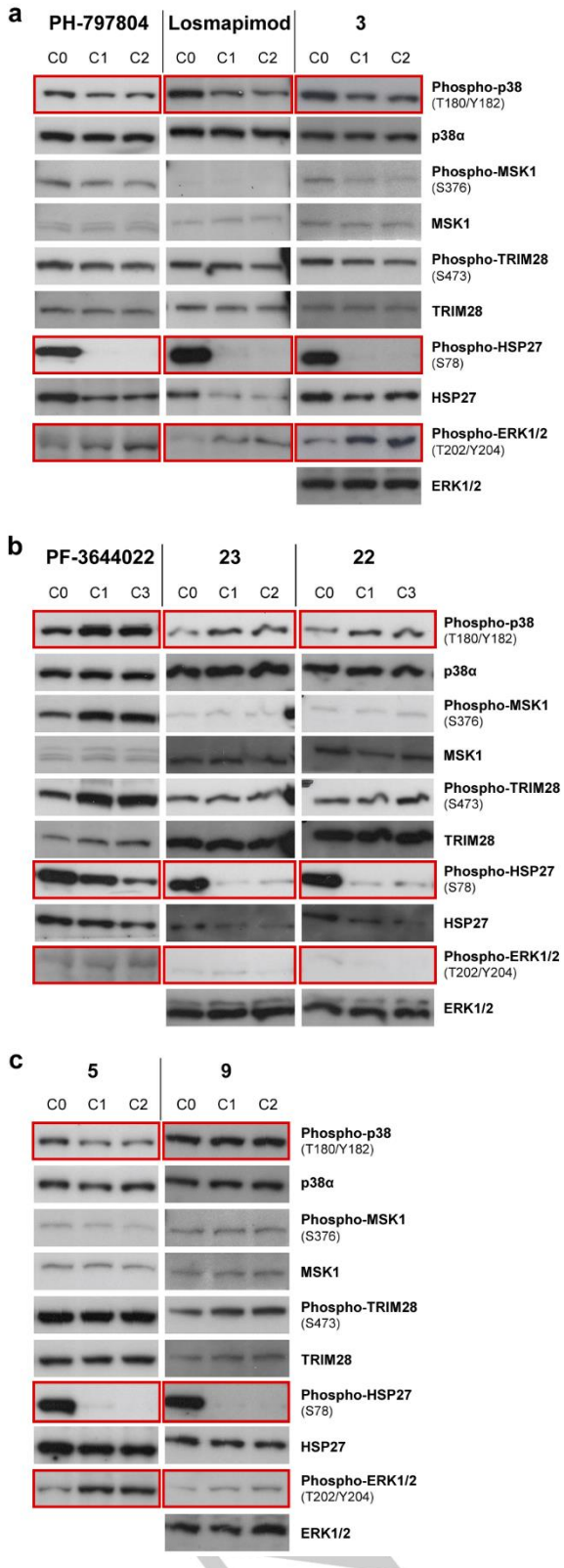

Figure 6. Immunoblots against proteins associated with p38 signaling in LPS-stimulated human PBMC in the presence of a) p38 inhibitors: PH-797804, losmapimod and compound **3**; b) MK2 inhibitors: PF-3644022, compound **23** and compound **22**; c) MK2 PoA inhibitors: compound **5** and compound **9**. Compound concentrations were chosen based on potencies observed for inhibition of TNF-α in LPS-stimulated human PBMC. C0: no compound, C1: IC80 from TNF-α assay, C2: 5xIC80 from TNF-α assay, C3: 4xIC80 from TNF-α assay. Phospho-p38, phospho-HSP27 and phospho-ERK1/2 are highlighted in red. The phosphorylated amino acid residues targeted by the anti-phospho primary antibodies are indicated. Representative immunoblots are shown for n=2 PBMC donors.

Further analysis of a number of compounds in the same series demonstrated that there is a disconnect between the in vitro PoA MK2 and MSK1 selectivity and the human PBMC data determining the downstream TNF-α and IL-10 release, respectively (Figure 7).

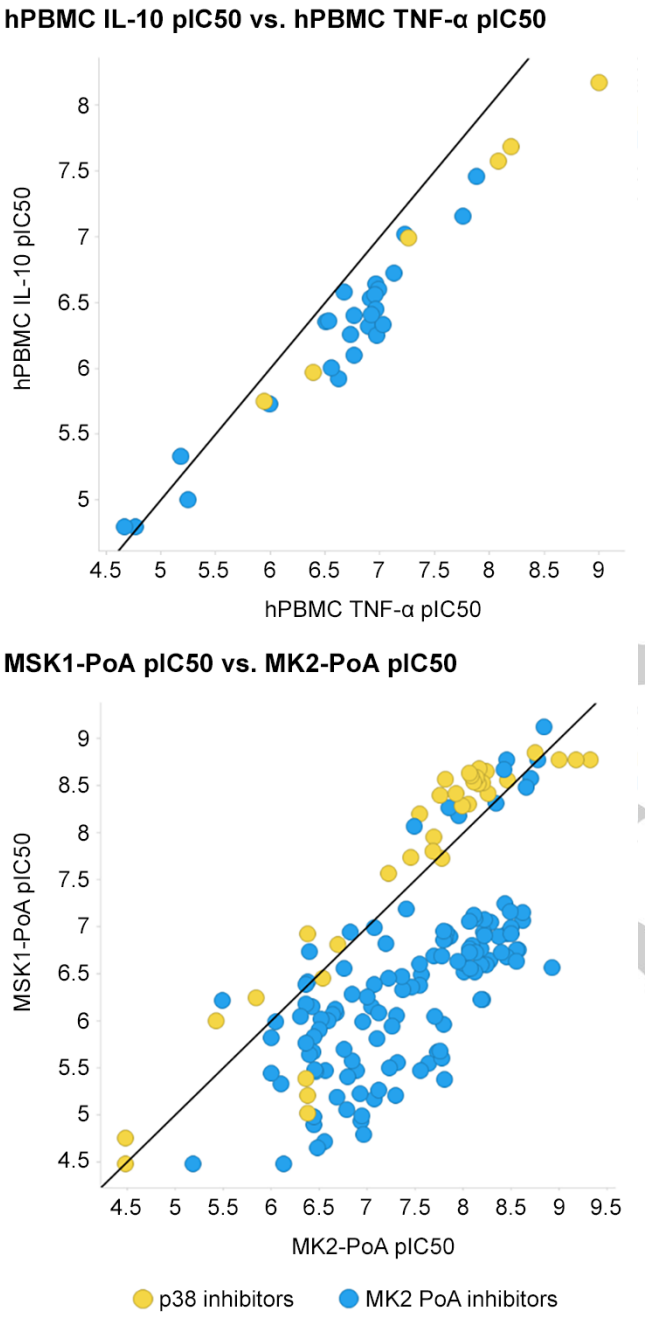

Figure 7. Plots of human PBMC IL-10 pIC50 vs. human PBMC TNF-α pIC50 and MSK1-prevention of activation (PoA) pIC50 vs. MK2-PoA pIC50. The line represents y = x. Shown are ATP competitive p38 inhibitors (yellow) and MK2 PoA inhibitors (blue).

This is an intriguing observation that supports a previous publication where substrate selective MK2 inhibitors were proposed to behave as p38 inhibitors in a cellular context due to differences in protein expression ([MK2]>[p38]),[24] causing all active p38 to be sequestered in an inactive complex with MK2 However, our data for PF-3644022 (Table 4) show that direct inhibition of MK2 also fails to preserve the anti-inflammatory IL-10 in human PBMC while inhibiting pro-inflammatory TNF-α production. Therefore, sequestration of p38 cannot be the only explanation for this and our data contradict previous literature reports.[2] More recent scientific reports[25],[26],[27],[28],[29],[30],[31] demonstrate that IL-10 is directly regulated by MK2 in addition to MSK1. As such, our data invalidate MK2 as a target for selective inhibition of inflammation.

Conclusions

In summary, by replacing the core pyrazole of compound **2** with imidazole, potency and solubility were improved within the series of compounds. The presence of dialkyl sulfonamide was essential to balance MK2 potency and selectivity, through its interaction with Asp168 in the p38α part of the p38α/MK2 complex. We discovered the highly selective compound **9** with a more than 200-fold selectivity of MK2-PoA over MSK1-PoA by extending towards the MK2 interface of the binding pocket. This unfortunately at the cost of oral drug properties, and thus our focus moved to other parts of the molecule. Supported by analysis of the central torsional angle, compound **18** was discovered, representing a novel series with increased potency and favorable physical chemistry properties. When we attempted to confirm this selectivity in the human PBMC cell assay, we found that selective inhibition of the MK2 activation did not preserve anti-inflammatory IL-10 while inhibiting pro-inflammatory TNF-α production. Using protein immunoblotting to explore the pathways around p38 confirmed that the majority of PoA MK2 compounds, despite their biochemical selectivity against MSK1 phosphorylation, behaved similarly to p38 inhibitors. This paper serves as a useful reminder that selectivity, as viewed from isolated enzyme assays, can be misleading, and selectivity should be viewed from the cellular context where proteins are in their native context and complete signaling pathways are intact. These data, along with the fact that selective inhibition of the MK2 activation did not preserve anti-inflammatory IL-10 production, led us to discontinue the project. Despite this, compounds **9** and **18** are useful tools for further research directed to understand the role of MK2 in the p38α signaling pathway.

Experimental Section

PoA MK2 enzyme assay

The kinase reaction takes place as a homogeneous assay in solution with purified recombinant proteins p-p38a and MK2. In this assay, MK2 is phosphorylated by active kinase p-p38a in vitro, phosphorylated MK2 is then captured by using NeutrAvidin coated ELISA plate and detected with a specific antibody directed towards the phosphorylated site (Thr222) of MK2. Compounds that prevent MK2 from phosphorylation by p-p38a lead to a decreased/no signal in an ELISA assay. Compounds are tested in IC_{50} format (10 concentrations: 33.3 µM to 1.7 nM).

Recombinant human MK2 was expressed in E. coli and purified in house Construct: His6-Avi(biotin)-hMK2[46-400], and was prepared as a 20 nM solution in assay buffer

PoA MSK1 enzyme assay

The kinase reaction takes place as a homogeneous assay in solution with purified recombinant proteins p-p38a and MSK1. In this assay, MSK1 is phosphorylated by active kinase p-p38a in vitro, phosphorylated MSK1 is then captured on ELISA plate by passive binding and detected with a specific antibody directed towards the phosphorylated site (Thr581) of MSK1 as illustrated in Figure 2. Compounds that prevent MSK1 from phosphorylation by p-p38α lead to a decreased/no signal in ELISA assay Compounds are tested in IC50 format (10 concentrations: 100 µM to 5.1 nM).

Human PBMC assay

Human PBMC were prepared from 150 ml of fresh whole blood per donor from healthy subjects. Informed consent was acquired from all subjects. In brief, fresh whole blood was layered on top of 15 ml Ficoll Paque PLUS (cat. 17-1440-03, Amersham) and centrifuged at 1600 rpm without brake for 35 mins at room temperature. The PBMC layer (second from top below the plasma layer) was collected by pipette and washed with at least 3 volumes R10 medium (RPMI 1640 w GlutaMax I + 25mM HEPES (500 ml) (cat. 72400-021, GIBCO) supplemented with heat inactivated FBS 10% (50 ml) (cat. 10438-026, GIBCO) and PEST (Penicillin+Steptomycin), (5 ml) (cat. 15070-063, GIBCO) and centrifuged at 1300 rpm for 10 minutes at room temperature. The supernatant was removed and the pellet resuspended in 1 ml phosphate buffered saline (PBS). Two ml of water was added to lyse red blood cells with gentle agitation by pipetting up and down for 30 seconds. The mixture was quenched by the addition of 2 ml 1.8% NaCl (sterile-filtered) and then further R10 buffer was added to fill the 50 ml Falcon tubes, which where centrifuged again. The cells were resuspended in fresh buffer and cells were pooled. The wash step was repeated. The cells were resuspended in 25 ml R10 buffer, diluted 1:10 in Trypan blue, and counted in a Bürker chamber. The cells were diluted to 1.052 x 10^6 cells /ml in prewarmed R10 buffer (200,000 cells /190 µl) and kept at 37°C. 1 µl compound/well was placed in 96-well round bottom culture plates (Costar 96 well Cell Culture Cluster, cat. 3799) and 190 ml cell solution was added and mixed at 300 rpm for 1 min, followed by preincubation for 45 minutes at 37°C, 5% CO_2. The experiment was initiated by the addition of 10 µl of 5 ng/ml LPS (from E.coli serotype 0127:B8, cat. L-4516, batch 109K4063) per well and incubated for 18 hours at 37°C, 5% CO_2. After the incubation the plate was centrifuged at 1200 rpm at 4°C and 160 µl cell-free supernatant was transferred to a V-bottomed 96-well plate (Greiner 96-well plates, cat. 651201) for cytokine analysis.

Cytokine V-plex MSD analysis

MSD kit with 96-well plates spotted with specific anti-cytokine capture antibodies, custom made by Meso Scale Discovery, was used. A combined working stock solution at 1 µg/ml of each cytokine was prepared. An 8-point cytokine calibration curve of 10000, 2500, 625, 156, 39, 9.8, 2.4 pg/ml and blank sample was prepared. For the assay the samples were thawed on ice. We added 25 µl/well calibrator or sample into each well. The plate was incubated at room temperature with shaking (600 rpm) for 2 hours. The plate was washed 3 x 300 ml with PBS-0.05% Tween-20 (PBS-Tween tablets cat. 09 9410-100, Medicago). For each plate used, we diluted a 60 µl aliquot of the stock detection antibody mix into 2.94 ml of Diluent 100 and this reagent was kept in the dark. We dispensed 25 µl/well detection antibody solution and incubated at room temperature with shaking for a further 2 hours. The plate was washed with 3 x 300 ml PBS-0.05% Tween-20. The read buffer was diluted 2-fold in deionized water to make a final concentration of 2x read buffer T, by using 10 ml of stock read buffer T (4x) and 10 ml deionized water for each plate and dispensed 150 µl/well 2x read buffer T and the plate was read on an MSD instrument.

Calculation of results

Calculations of results were done in Excel. XLfit was used to fit the calibrator data to a standard curve, from which the concentration of each cytokine was calculated using the following equation: % Inhibition = 100 x [(max-X)/(max-min)], where X = cytokine concentration for each compound concentration, Max = average value cytokine conc pos controls (+ LPS), Min = average value cytokine conc neg controls (- LPS). We used XLfit to calculate the results, inhibition method 203 is recommended. Active compounds were defined as compounds with ≥30% inhibition. Incomplete curves with inhibition >50% were extrapolated by locking the max value to 100.

Protein immunoblot analysis

8 x 10^6 PBMC isolated from freshly drawn blood from healthy volunteers were placed in 35 mm dishes (Corning) in RPMI1640 medium (cat. # 11875-093, Thermo Fisher, Waltham, MA, USA) supplemented with 10% heat inactivated fetal bovine serum (cat. 10082-147, Thermo Fisher, Waltham, MA, USA), incubated with the designated compounds or DMSO for 45 min, followed by an incubation with 0.5 ng/ml LPS (cat. L4516 Sigma Aldrich, St. Louis, MO, USA) for 30 min. Both incubations were done at 37˚C in a 5% CO2 incubator. The cells were then centrifuged at 1000 g and 4°C for 2 minutes and lysed on ice with lysis buffer (20 mM Tris (pH 7.2), 1 mM EDTA, 1 mM EGTA, 5 mM sodium pyrophosphate, 1 mM sodium orthophosphate, 50 mM sodium fluoride, 270 mM sucrose and 1% Triton X-100) supplemented with Complete Mini Protease Inhibitor Cocktail tablets (cat. 11836153001, Roche, Switzerland). The lysates were centrifuged at 21 000 g at 4°C for 10 min and protein concentrations in the supernatants were measured using a BCA protein assay kit (cat. 23225, Thermo Fisher). The proteins were then separated by SDS-PAGE on NuPAGE Novex 4-12% Bis-Tris gels (cat. NP0321BOX, Thermo Fisher) and transferred to PVDF membranes using the iBlot system (Thermo Fisher). Following blocking in TBS-Tween with 5% BSA, the membranes were incubated with the following antibodies at 4°C overnight with constant agitation: phospho-p38 (pT180/pY182) antibody (cat. 4511, Cell Signaling Technology, Boston, MA, USA), 1:2500; phospho-MSK1 (pS376) antibody (cat. 9591, Cell Signaling Technology, Boston, MA, USA), 1:500; phospho-HSP27 (pS78) antibody (cat. 1543-1, Epitomics, Burlingame, CA, USA), 1:2000; phospho-TRIM28 (pS473) antibody (cat. ab109545, Abcam, Cambridge, UK), 1:20000; phospho-ERK (p44/p42) (pT202/pY204) antibody (cat. 4376, Cell Signaling Technology, Boston, MA, USA), 1:1000. After washing of the membranes 3 times in TBS-Tween, they were incubated with an HRP-conjugated anti-rabbit IgG antibody at RT for 1 hour with constant agitation. Following 3 more washes in TBS-Tween, the chemiluminescence was developed in a freshly made solution containing 2.5 mM luminol, 200 µM coumaric acid, 0.018% hydrogen peroxide and 100 mM Tris (pH 8.6), and the signal was transferred to an X-ray film. The membranes were stripped of all antibodies by incubation in a solution containing 2% SDS, 100 mM 2-mercaptoethanol and 62.5 mM Tris (pH 6.7) at 60°C for 30 minutes. After 2 washes in distilled water and 3 washes in TBS-Tween, the membranes were incubated with the following antibodies at 4°C overnight with constant agitation: p38α/MAPK14 antibody (cat. AF8691, R&D Systems, Minneapolis, MN, USA), 1:2000; MSK1 antibody (cat. 3489, Cell Signaling Technology, Boston, MA, USA), 1:2500; HSP27 antibody (cat. 2402, Signaling Technology, Boston, MA, USA), 1:2000; TRIM28 antibody (cat. ab109287, Abcam, Cambridge, UK), 1:10000; ERK (p44/p42) antibody (cat. 4695, Cell Signaling Technology, Boston, MA, USA), 1:1000. As described above, the membranes were again washed, probed with secondary HRP-conjugated antibodies (anti-mouse IgG for the HRP27 antibody and anti-rabbit IgG for the other antibodies) and the chemiluminescence was developed.

Supporting Information

The supporting information contains synthetic procedures and analytical characterization for all new compounds described in this paper, rat pharmacokinetic data for **18** and pan-kinase selectivity data for **9** and **18**.

Keywords: kinase inhibitor • mode of action • prevention of activation • ligand design • drug discovery

Table of Contents

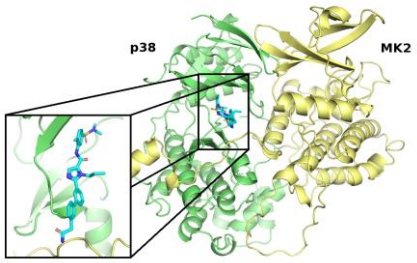

The p38α pathway is an attractive target for inflammation research. Cellular signaling downstream of p38α was probed using optimized pyrazole amide MK2 prevention of activation (PoA) inhibitors. Despite biochemical selectivity blocking p38 phosphorylation of MK2 vs MSK1, in cells PoA MK2 and p38 inhibitors behaved similarly. This study highlights the importance of selective tool compounds in untangling complex cellular signaling pathways.

References

1 S. Duraisamy, M. Bajpai, U. Bughani, S.G. Dastidar, A. Ray, P. Chopra, *Expert Opin. Ther. Targets* **2008**, *12*, 921 – 936.

2 M. Gaestel, A. Kotlyarov, M. Kracht, *Nat. Rev. Drug Discovery* **2009**, *8*, 480 – 499.

3 M. Fiore, S. Forli, F. Manetti, *J. Med. Chem.* **2016**, *59*, 3609 − 3634.

4 J. Regan, S. Breitfelder, P. Cirillo, T. Gilmore, A.G. Graham, E. Hickey, B. Klaus, J. Madwed, M. Moriak, N. Moss, C. Pargellis, S. Pav, A. Proto, A. Swinamer, L. Tong, C. Torcellini, *J. Med. Chem.* **2002**, *45*, 2994 – 3008.

5 J.P. Duffy, E.M. Harrington, F.G. Salituro, J.E. Cochran, J. Green, H. Gao, G.W. Bemis, G. Evindar, V.P. Galullo, P.J. Ford, U.A. Germann, K.P. Wilson, S.F. Bellon, G. Chen, P. Taslimi, P. Jones, C. Huang, S. Pazhanisamy, Y. Wang, M.A. Murcko, M.S.S. Su, *ACS Med. Chem. Lett.* **2011**, *2*, 758 – 763.

6 C. Ding, *Curr. Opin. Investig. Drugs* **2006**, *7*, 1020 − 1025.

7 M.C. Genovese, *Arthritis Rheum.* **2009**, *60*, 317 – 320.

8 J.C.S. Arthur, S.C. Ley, *Nat. Rev. Immunol.* **2013**, *13*, 679 – 692.

9 J.G. Cumming, J.E. Debreczeni, F. Edfeldt, E. Evertsson, M. Harrison, G.A. Holdgate, M.J. James, S.G. Lamont, K. Oldham, J.E. Sullivan, S.J. Wells, *J. Med. Chem.* **2015**, *58*, 278 − 293.

10 W. Davidson, L. Frego, G.W. Peet, R.R. Kroe, M.E. Labadia, S.M. Lukas, R.J. Snow, S. Jakes, C.A. Grygon, C. Pargellis, B.G. Werneburg, *Biochemistry* **2004**, *43*, 11658 – 11671.

11 J. Das, R.V. Moquin, A.J. Dyckman, T. Li, S. Pitt, R. Zhang, D.R. Shen, K.W. McIntyre, K. Gillooly, A.M. Doweyko, J.A. Newitt, J.S. Sack, H. Zhang, S. E. Kiefer, K. Kish, M. McKinnon, J.C. Barrish, J.H. Dodd, G.L. Schieven, K. Leftheris, *Bioorg. Med. Chem. Lett.* **2010**, *20*, 6886 − 6889.

12 Small-Molecule Drug Discovery Suite 2014-2: Glide, version 6.3, Schrödinger, LLC, New York, NY, **2014**.

13 Jaguar, version 8.4, Schrödinger, LLC, New York, NY, **2014**.

14 F.M. Gurgis, W. Ziaziaris, L. Munoz, *Mol. Pharmacol.* **2014**, *85*, 345 – 356.

15 S. Kostenko, U. Moens, *Cell. Mol. Life Sci.* **2009**, *66*, 3289 – 3307.

16 K. Singh, M. Cassano, E. Planet, S. Sebastian, S.M. Jang, G. Sohi, H. Faralli, J. Choi, H.D. Youn, F.J. Dilworth, D. Trono, *Genes Dev.* **2015**, *29*, 513 – 525.

17 S.R. Selness, R.V. Devraj, B. Devadas, J.K. Walker, T.L. Boehm, R.C. Durley, H. Shieh, L. Xing, P.V. Rucker, K.D. Jerome, A.G. Benson, L.D. Marrufo, H.M. Madsen, J. Hitchcock, T.J. Owen, L. Christie, M.A. Promo, M, B.S. Hickory, E. Alvira, W. Naing, R. Blevis-Bal, D. Messing, J. Yang, M.K. Mao, G. R. Yalamanchili, R.V. Embse, J. Hirsch, J.; M. Saabye, S. Bonar, E. Webb, G. Anderson, J.B. Monahan, *Bioorg. Med. Chem. Lett.* **2011**, *21*, 4066 – 4071.

18 N.M. Aston, P. Bamborough, J.B. Buckton, C.D. Edwards, D.S. Holmes, K.L. Jones, V.K. Patel, P.A. Smee, D.O. Somers, G. Vitulli, A.L. Walker, *J. Med. Chem.* **2009**, *52*, 6257 – 6269.

19 D.R. Anderson, M.J. Meyers, R.G. Kurumbail, N. Caspers, G.I. Poda, S.A. Long, B.S. Pierce, M.W. Mahoney, R.J. Mourey, M.D. Parikh, *Bioorg. Med. Chem. Lett.* **2009**, *19*, 4882 – 4884.

20 X. Huang, X. Zhu, X. Chen, W. Zhou, D. Xiao, S. Degrado, R. Aslanian, J. Fossetta, D. Lundell, D.; F. Tian, P. Trivedi, A. Palani, *Bioorg. Med. Chem. Lett.* **2012**, *22*, 65 – 70.

21 D. Xiao, A. Palani, X. Huang, M. Sofolarides, W. Zhou, X. Chen, R. Aslanian, Z. Guo, J. Fossetta, F. Tian, P. Trivedi, P. Spacciapoli, C.E. Whitehurst, D. Lundell, *Bioorg. Med. Chem. Lett.* **2013**, *23*, 3262 – 3266.

22 X. Gong, X. Ming, P. Deng, Y. Jiang, *J. Cell. Biochem.* **2010**, *110*, 1420 – 1429.

23 R. Ben-Levy, S. Hooper, R. Wilson, H.F. Paterson, C.J. Marshall, *Curr. Biol.* **1998**, *8*, 1049 – 1057.

24 B.S. Hendriks, K.M. Seidl, J.R. Chabot, *BMC Syst. Biol.* **2010**, *4*, 1 – 17.

25 K. Soukup, A. Halfmann, M. Le Bras, E. Sahin, S. Vittori, F. Poyer, C. Schuh, R. Luger, B. Niederreiter, T. Haider, D. Stoiber, S. Blüml, G. Schabbauer, A. Kotlyarov, M. Gaestel, T. Felzmann, A.M. Dohnal, *J. Immunol.* **2015**, *195*, 541 – 552.

26 C. Ehlting, M. Trilling, C. Tiedje, A. Zimmermann, V.T.K. Le, M. Gaestel, H. Hengel, D. Häussinger, J.G. Bode, Z. *Gastroenterol.* **2014**, *52*, 5 – 48.

27 C. Ehlting, N. Ronkina, O. Böhmer, U. Albrecht, K.A. Bode, K.S. Lang, A. Kotlyarov, D. Radzioch, M. Gaestel, D. Häussinger, J.G. Bode, *J. Biol. Chem.* **2011**, *286*, 24113 – 24124.

28 J. Fricke, P.L. Collins, L.Y. Koo, C.R. Brown, *J. Virol.* **2013**, *87*, 1333 – 47.

29 A.J. Guess, R. Ayoob, R.; Chanley, M.; Manley, J.; Agrawal, S.; Pengal, R.; Becknell, B.; Benndorf, R.; Smoyer, W.E.; Cajaiba, M.M.; Pyle, A.L.; Kopp, J.B.; Ronkina, N.; Gaestel, M.; Benndorf, R.; Smoyer, W.E. *PLoS One* **2013**, *8*, e54239.

30 K.F. Mackenzie, M.J. Pattison, J.S.C. Arthur, *Crit. Rev. Immunol.* **2014**, *34*, 315 – 345.

31 C. Olaisen, R. Müller, A. Nedal, M. Otterlei, *Cell. Signalling* **2015**, *27*, 1478 – 1487.